



OPEN

Functional roles of multiple Ton complex genes in a *Sphingobium* degrader of lignin-derived aromatic compounds

Masaya Fujita^{1,4}, Shodai Yano¹, Koki Shibata¹, Mizuki Kondo², Shojiro Hishiyama³, Naofumi Kamimura¹ & Eiji Masai¹

TonB-dependent transporters (TBDTs) mediate outer membrane transport of nutrients using the energy derived from proton motive force transmitted from the TonB–ExbB–ExbD complex localized in the inner membrane. Recently, we discovered *ddvT* encoding a TBDT responsible for the uptake of a 5,5-type lignin-derived dimer in *Sphingobium* sp. strain SYK-6. Furthermore, overexpression of *ddvT* in an SYK-6-derivative strain enhanced its uptake capacity, improving the rate of platform chemical production. Thus, understanding the uptake system of lignin-derived aromatics is fundamental for microbial conversion-based lignin valorization. Here we examined whether multiple *tonB*-, *exbB*-, and *exbD*-like genes in SYK-6 contribute to the outer membrane transport of lignin-derived aromatics. The disruption of *tonB2–6* and *exbB3* did not reduce the capacity of SYK-6 to convert or grow on lignin-derived aromatics. In contrast, the introduction of the *tonB1–exbB1–exbD1–exbD2* operon genes into SYK-6, which could not be disrupted, promoted the conversion of β -O-4-, β -5-, β -1-, β - β -, and 5,5-type dimers and monomers, such as ferulate, vanillate, syringate, and protocatechuate. These results suggest that TonB-dependent uptake involving the *tonB1* operon genes is responsible for the outer membrane transport of the above aromatics. Additionally, *exbB2/tolQ* and *exbD3/tolR* were suggested to constitute the Tol-Pal system that maintains the outer membrane integrity.

Lignin, a major component of plant cell walls, is the most abundant aromatic compound on Earth and is expected to be a renewable alternative to fossil resources^{1,2}. Recently, the production of value-added chemicals from lignin by combining chemical depolymerization of lignin with bacterial catabolic systems for low-molecular-weight aromatic compounds has attracted much attention³. Many bacteria catabolizing lignin-derived aromatic compounds have been identified, and their catabolic enzyme genes have been characterized. These genes are useful for the production of value-added chemicals from heterogeneous lignin-derived aromatic compounds⁴. For example, *Sphingobium* sp. strain SYK-6, an alphaproteobacterium, is a model strain capable of catabolizing various lignin-derived aromatic dimers and monomers and produces 2-pyrone-4,6-dicarboxylic acid (PDC), a platform chemical for the synthesis of functional polymers as an intermediate^{5,6}. A significant portion of the SYK-6 genes involved in the catabolism of lignin-derived aromatic compounds have been characterized, and PDC production systems using these genes have been developed^{4,7}. Recently, transporter genes for lignin-derived aromatic compounds have also been studied to improve their uptake capacity^{8,9}. However, uptake systems, especially uptake across the outer membrane, remain largely unexplored.

The outer membrane transport by Gram-negative bacteria is mediated by porins, substrate-specific channels, and TonB-dependent transporters (TBDTs)¹⁰. Porins and substrate-specific channels are responsible for non-specific and specific passive transport, respectively. TBDTs are active transporters that specifically transport relatively large compounds, such as siderophores and vitamin B12, using the energy derived from proton motive force transmitted from the TonB–ExbB–ExbD complex (Ton complex) localized in the inner membrane^{11–13}. Since most bacteria have only a few *tonB*-like genes compared to the number of TBDT-like genes, one TonB likely interacts with multiple TBDTs to transfer the energy required for substrate uptake^{14,15}. In addition to the

¹Department of Bioengineering, Nagaoka University of Technology, Nagaoka, Niigata 940-2188, Japan. ²Center for Integrated Technology Support, Nagaoka University of Technology, Nagaoka, Niigata, Japan. ³Forestry and Forest Products Research Institute, Tsukuba, Ibaraki, Japan. ⁴Present address: Structural Biology Research Center, Institute of Materials Structure Science, High Energy Accelerator Research Organization (KEK), Tsukuba, Ibaraki, Japan. ✉email: emasai@vos.nagaokaut.ac.jp

above substrates, the involvement of TBDTs in the uptake of oligopeptides, saccharides, and metal ions has been demonstrated, thus, expanding the range of substrates transported by TBDTs^{16–18}. It is also known that *tolA*, *tolQ*, and *tolR*, homologs of *tonB*, *exbB*, and *exbD*, respectively, constitute the Tol-Pal system, stabilizing the outer membrane structure and is involved in the septum formation during cell division¹⁹. The introduction of *tolQ* and *tolR* into *exbB* and *exbD* mutants of *Escherichia coli* restored the ability of these mutants to take up group B colicin, indicating that *tolQ* and *tolR* can partially complement the functions of *exbB* and *exbD*, respectively²⁰.

The outer membrane transport of aromatic compounds used as carbon and energy sources is mediated by passive transporters, such as the vanillate specific-channel OpdK of *Pseudomonas aeruginosa* PAO1 and naphthalene porin OmpW of *Pseudomonas fluorescens*^{21,22}. However, SYK-6 has no OpdK-like genes and only one gene that shows similarity with the known aromatic compound porin (*ompW*)^{21,23}, but instead has 74 TBBDT-like genes²⁴. Recently, we have demonstrated that a TBBDT (DdvT) mediates the uptake of 5,5'-dehydrodivanillate (DDVA), a lignin-derived 5,5-type dimer, across the outer membrane in SYK-6. When *ddvT* was overexpressed in an SYK-6 mutant of the PDC hydrolase gene, the PDC production rate improved. Therefore, overexpression of TBBDT genes seems effective in improving the efficiency of microbial conversion. Additionally, the Ton complex composed of TonB1–ExbB1–ExbD1–ExbD2 was suggested to be involved in the uptake of DDVA mediated by DdvT. The phylogenetic analysis of 74 TBBDT-like genes in SYK-6 with known TBBDT genes revealed that 53 TBBDT-like genes form two phylogenetically distinct clades from known TBBDT genes. Among them, the expression of 12 TBBDT genes in SYK-6 was specifically induced by lignin-derived aromatic compounds. These facts suggest that the Ton system, consisting of TBBDTs and Ton complex, plays a vital role in the uptake of lignin-derived aromatic compounds by SYK-6 across the outer membrane. Additionally, the genomes of strains of Sphingomonadaceae, which include many strains capable of degrading recalcitrant aromatic compounds, contain many TBBDT-like genes, suggesting that the Ton system is involved in the outer membrane transport of these aromatic compounds²⁵. A recent study strongly suggests that TBBDTs are involved in the uptake of aromatic compounds, such as benzo[a]pyrene in *Novosphingobium pentaromativorans* US6-1, which degrades polyaromatic hydrocarbons²⁶.

This study investigated whether the Ton system is involved in the outer membrane transport of lignin-derived aromatic compounds in SYK-6 by analyzing disruption and overexpression strains of genes presumed to encode components of the Ton complex. Additionally, we predicted the Tol-Pal system genes, which contributed to the stabilization of the outer membrane and characterized their mutants.

Results and discussion

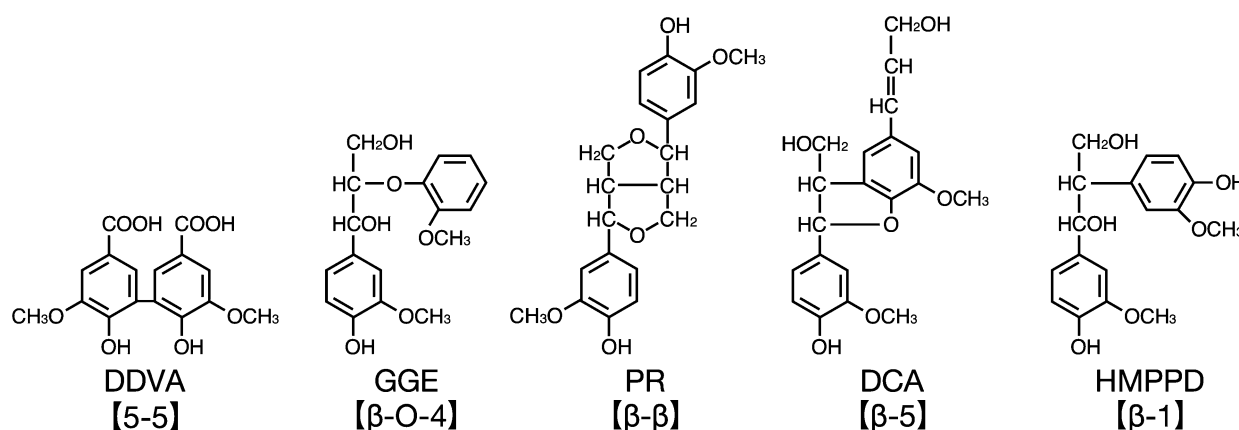
The *ompW*-like gene is not required for the conversion of lignin-derived aromatic compounds. SLG_38320 (*ompW*) of SYK-6 shows similarity with known aromatic compound porins (*ompW* family proteins; 30% identity with P0A915 of *Escherichia coli*)^{21,23,24}. In our previous study, *ompW* mutant ($\Delta ompW$) exhibited comparable growth to the wild type in Wx medium containing 5 mM DDVA, ferulate (FA), vanillin (VN), vanillate (VA), syringaldehyde (SN), syringate (SA), or protocatechuate (PCA)²⁴. Here to clarify whether *ompW* is involved in the uptake of lignin-derived aromatic compounds, we used the resting cells of $\Delta ompW$ to measure their capacity to convert lignin-derived 5,5-, β -O-4-, β - β -, β -5-, and β -1-type dimers [DDVA, guaiacylglycerol- β -guaiacyl ether (GGE), pinoresinol (PR), dehydrodiconiferyl alcohol (DCA), and 1,2-bis(4-hydroxy-3-methoxyphenyl)-propane-1,3-diol (HMPPD), respectively] and monomers [acetovanilone (AV), FA, VN, VA, SN, SA, and PCA] (Figs. 1, S1). No reduction in the conversion capacity of $\Delta ompW$ compared to the wild type was observed, indicating that *ompW* is unnecessary to uptake lignin-derived aromatic compounds tested in this study.

The growth of *tonB* mutants on lignin-derived aromatic compounds and their conversion capacity. SYK-6 has six *tonB*-like genes (SLG_14430 [*tonB1*], SLG_34540 [*tonB2*], SLG_36940 [*tonB3*], SLG_37490 [*tonB4*], SLG_01650 [*tonB5*], and SLG_14690 [*tonB6*]), three *exbB*-like genes (SLG_14440 [*exbB1*], SLG_02500 [*exbB2/tolQ*], and SLG_10800 [*exbB3*]), and three *exbD*-like genes (SLG_14450 [*exbD1*], SLG_14460 [*exbD2*], and SLG_02490 [*exbD3/tolR*]) (Table 1, Fig. S2)²⁴. Our previous mutant analysis showed that *tonB2*–6 were not involved in the uptake of DDVA²⁴. *tonB1* that constitutes the *tonB1* operon (*tonB1*–*exbB1*–*exbD1*–*exbD2*) could not be disrupted, implying that *tonB1* is essential for the growth of SYK-6^{24,27}. *tonB2* and *fiuA* encoding a TBBDT located immediately downstream of *tonB2* play a major role in iron acquisition across the outer membrane of SYK-6²⁷. Therefore, the growth capacity of *tonB2* mutant ($\Delta tonB2$) was reduced on various carbon sources^{24,27}.

To examine the involvement of *tonBs* in the uptake of lignin-derived aromatic compounds, we measured the growth of *tonB3 tonB4 tonB5 tonB6* quadruple mutant ($\Delta tonB3456$) and its *tonB2* mutant ($\Delta tonB23456$) in Wx medium containing 5 mM FA, VN, VA, SA, or PCA, or Wx medium containing SEMP (10 mM sucrose, 10 mM glutamate, 0.13 mM methionine, and 10 mM proline). We also evaluated the capacity of resting cells of $\Delta tonB3456$ and $\Delta tonB23456$ to convert GGE, PR, DCA, HMPPD, AV, FA, VN, VA, SN, SA, and PCA. $\Delta tonB3456$ and $\Delta tonB23456$ showed no reduction in growth on all carbon sources compared with wild type and $\Delta tonB2$, respectively (Fig. S3). Additionally, the conversion capacity of $\Delta tonB3456$ and $\Delta tonB23456$ to each compound was not reduced compared to the wild type (Fig. 2). These results suggest that *tonB2*–6 are not involved in the uptake of these lignin-derived aromatic compounds tested in this study.

The growth of *exbB* and *exbD* mutants on lignin-derived aromatic compounds. We tried disrupting three *exbB*-like genes and three *exbD*-like genes and finally obtained *exbB2/tolQ*, *exbB3*, and *exbD3/tolR* mutants (Table 1, Fig. S4). *exbB1*, *exbD1*, and *exbD2*, which form the *tonB1* operon, could not be disrupted, suggesting that this operon plays an essential role in the growth of SYK-6. We measured the growth of *exbB2/tolQ* mutant ($\Delta exbB2/tolQ$), *exbB3* mutant ($\Delta exbB3$), and *exbD3/tolR* mutant ($\Delta exbD3/tolR$) in Wx medium contain-

Lignin-derived dimers



Lignin-derived monomers

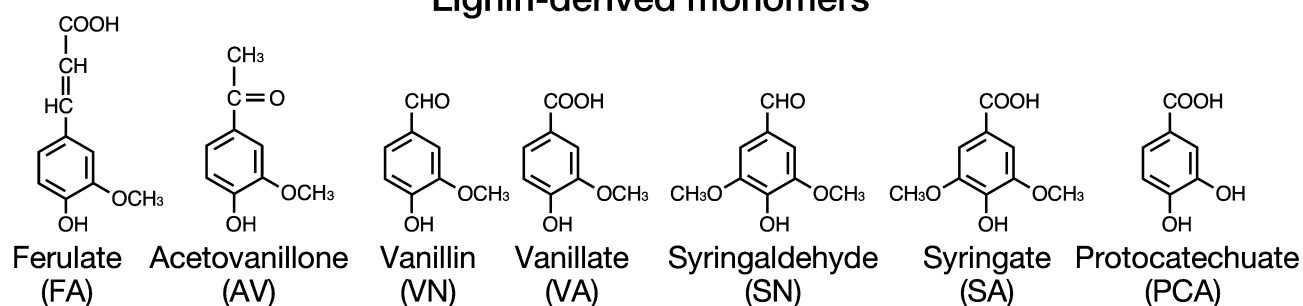


Figure 1. Chemical structures of lignin-derived dimers and monomers used in this study. DDVA, 5,5'-dehydrodivanillate; GGE, guaiacylglycerol-β-guaiacyl ether; PR, pinoresinol; DCA, dehydrodiconiferyl alcohol; HMPPD, 1,2-bis(4-hydroxy-3-methoxyphenyl)-propane-1,3-diol. This figure was generated using Canvas X Draw version 7.0.2. (<https://www.canvasgfx.com/products/canvas-x-draw>).

Locus tag	Putative function	Most similar protein ^a	Annotation	Strain	Sequence identity (%)	E-value
TonB						
SLG_01650 (<i>tonB5</i>)	TonB	–	–	–	–	–
SLG_14430 (<i>tonB1</i>)	TonB	–	–	–	–	–
SLG_14690 (<i>tonB6</i>)	TonB	–	–	–	–	–
SLG_34540 (<i>tonB2</i>)	TonB	–	–	–	–	–
SLG_36940 (<i>tonB3</i>)	TonB	–	–	–	–	–
SLG_37490 (<i>tonB4</i>)	TonB	–	–	–	–	–
ExbB						
SLG_02500 (<i>exbB2/tolQ</i>)	ExbB/TolQ	P50598	Tol-Pal system protein TolQ	<i>Pseudomonas aeruginosa</i> PAO1	41	4E–46
SLG_10800 (<i>exbB3</i>)	ExbB	–	–	–	–	–
SLG_14440 (<i>exbB1</i>)	ExbB	P0C7L9	Biopolymer transport protein ExbB	<i>Xanthomonas campestris</i> pv <i>campestris</i> str. ATCC33913	38	4E–42
ExbD						
SLG_02490 (<i>exbD3/tolR</i>)	ExbD/TolR	P0ABV2	Biopolymer transport protein ExbD	<i>Escherichia coli</i> K-12	41	7E–27
SLG_14450 (<i>exbD1</i>)	ExbD	P0C7I9	Biopolymer transport protein ExbD2	<i>Xanthomonas campestris</i> pv <i>campestris</i> str. ATCC33913	29	6E–17
SLG_14460 (<i>exbD2</i>)	ExbD	P0C7M0	Biopolymer transport protein ExbD1	<i>Xanthomonas campestris</i> pv <i>campestris</i> str. ATCC33913	37	3E–24

Table 1. Candidate genes encoding the Ton complex components in *Sphingobium* sp. strain SYK-6. ^aMost similar proteins were searched in the Swiss-Prot database using the BLAST-P program⁴⁰ and not displayed if the E-value is greater than 1e-10.

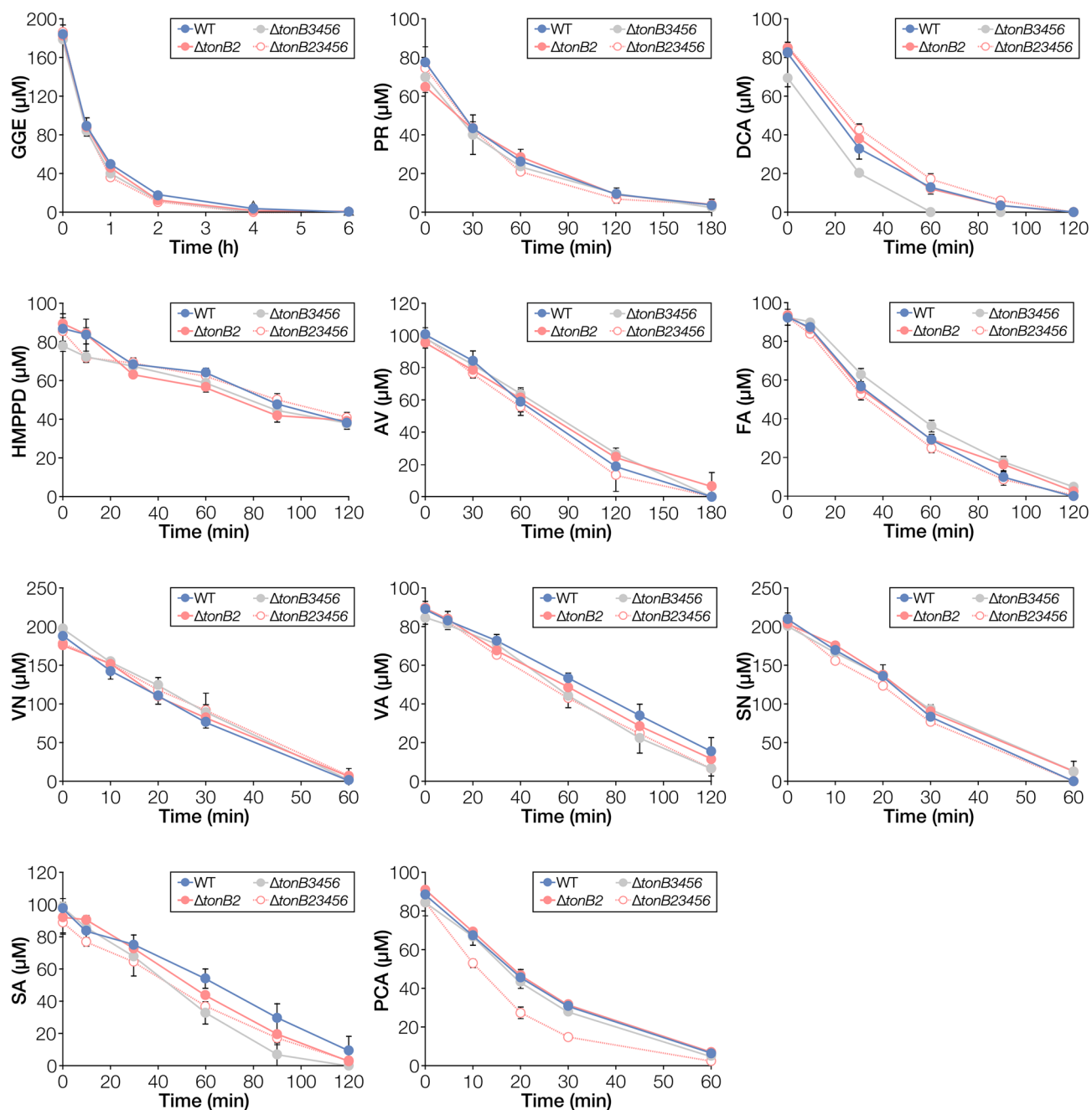


Figure 2. Conversion of lignin-derived aromatic compounds by resting cells of *tonB* multiple mutants. Cells of SYK-6, $\Delta tonB2$, $\Delta tonB3456$, and $\Delta tonB23456$ were incubated with 200 μM GGE, 100 μM PR, 100 μM DCA, 100 μM HMPPD, 100 μM AV, 100 μM FA, 200 μM VN, 100 μM VA, 200 μM SN, 100 μM SA, or 100 μM PCA. Portions of the reaction mixtures were collected, and the amount of substrate was measured using HPLC. Each value is the average \pm the standard deviation of three independent experiments. This figure was generated using Canvas X Draw version 7.0.2. (<https://www.canvasgfx.com/products/canvas-x-draw>).

ing FA, VN, VA, SA, PCA, or SEMP or diluted LB (Fig. 3). $\Delta exbB3$ exhibited the same level of growth as the wild type on all substrates. In contrast, the growth of $\Delta exbB2/tolQ$ and $\Delta exbD3/tolR$ was significantly reduced or defective in SEMP, diluted LB, and lignin-derived aromatic compounds except for FA. The growth was restored when the plasmids carrying *exbB2/tolQ* and *exbD3/tolR* were introduced into $\Delta exbB2/tolQ$ and $\Delta exbD3/tolR$, respectively (Figs. S5, S6). Therefore, growth retardation or defect was due to the disruption of *exbB2/tolQ* and *exbD3/tolR*. However, the introduction of *exbB1* into $\Delta exbB2/tolQ$ and *exbD1-exbD2* into $\Delta exbD3/tolR$ did not restore their growth (Figs. S5, S6). These results indicate that *exbB1* and *exbD1/exbD2* cannot replace the functions of *exbB2/tolQ* and *exbD3/tolR*, respectively.

exbB2/tolQ and *exbD3/tolR* were located just upstream of *tolA*, *tolB*, and *pal*-like genes that constitute the Tol-Pal system (Fig. S2), which plays essential roles in the stabilization of the outer membrane structure and

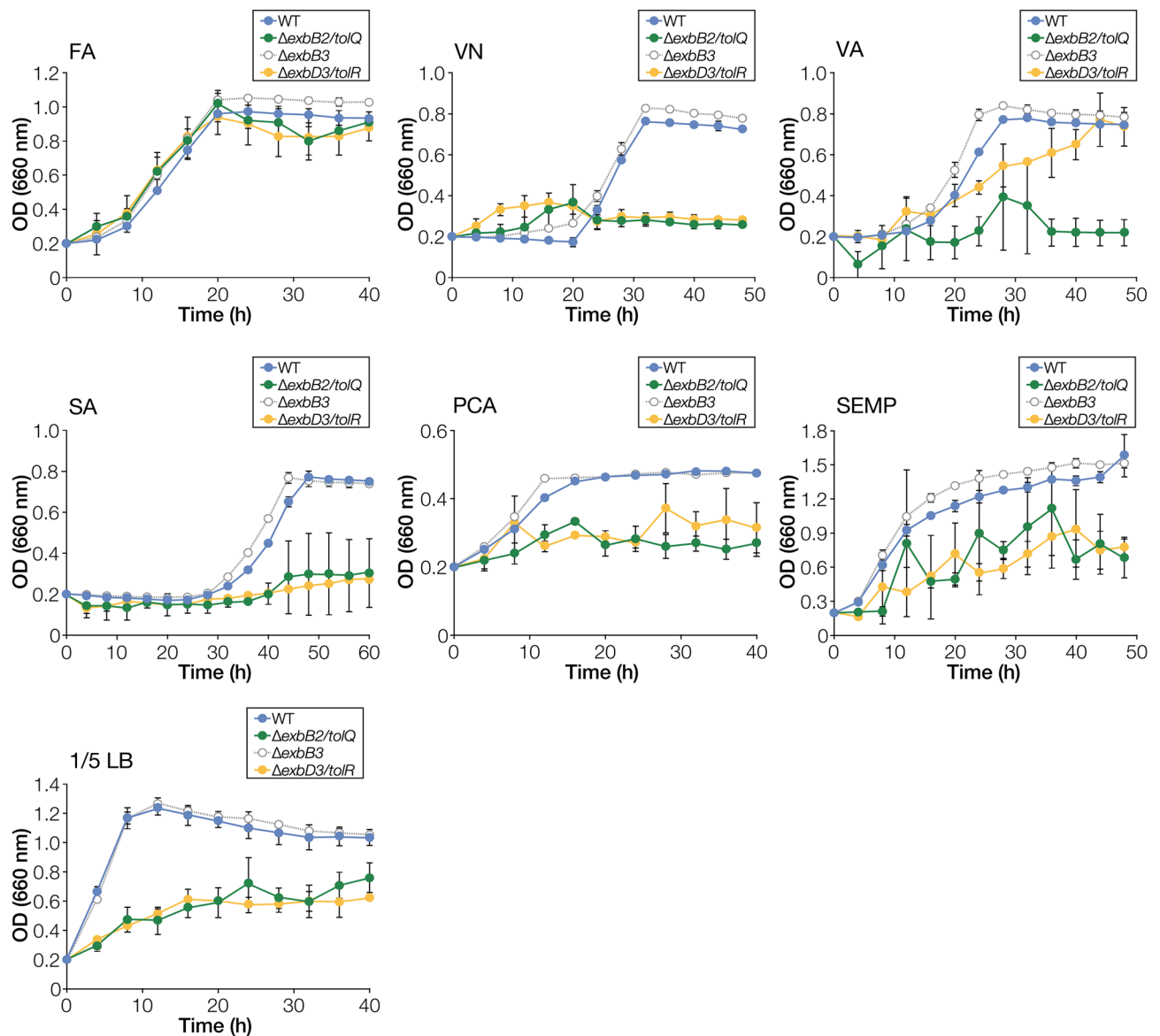


Figure 3. Growth of *exbB* and *exbD* mutants on lignin-derived aromatic compounds. Cells of SYK-6, $\Delta exbB2/tolQ$, $\Delta exbB3$, and $\Delta exbD3/tolR$ were cultured in Wx medium containing 5 mM FA, VN, VA, SA, or PCA, Wx medium containing SEMP, and diluted LB (1/5 LB). Cell growth was monitored by measuring the OD₆₆₀. Each value is the average \pm the standard deviation of three independent experiments. This figure was generated using Canvas X Draw version 7.0.2. (<https://www.canvasgfx.com/products/canvas-x-draw>).

septum formation during cell division. Additionally, *ybgC*, whose relevance to the Tol-Pal system is unknown, was found immediately upstream of *exbB2/tolQ*^{19,28}. Since a similar set of genes (*ybgC-tolQ-tolR-tolA-tolB-pal*) has been found in many bacteria as the genes encoding the Tol-Pal system²⁹, *exbB2/tolQ* and *exbD3/tolR* are likely components of the Tol-Pal system. Therefore, disruption of these genes is presumed to have caused instability of the outer membrane and associated growth retardation and defects on various carbon sources. The details of the characterization of $\Delta exbB2/tolQ$ and $\Delta exbD3/tolR$ will be described later.

In ExbB and TolQ of *E. coli*, Thr-148 and Thr-181 (ExbB numbering) are essential for proton translocation and Glu-176 (ExbB numbering) whose function is unclear but essential, are conserved^{30,31}. These amino acid residues were conserved in ExbB1 and ExbB2/TolQ of SYK-6 (Fig. S7A). However, Glu-176 is not conserved in ExbB3 of SYK-6. With the fact that the growth capacity of $\Delta exbB3$ was not reduced on each carbon source compared to the wild type (Fig. 3), likely, ExbB3 does not function as ExbB. In contrast, Asp-25 (ExbD numbering) essential for acquiring proton motive force by ExbD and TolR in *E. coli* was conserved among ExbD1, ExbD2, and ExbD3/TolR of SYK-6 (Fig. S7B).

The effect of overexpression of the *tonB1* operon genes on the conversion of lignin-derived aromatic compounds. To examine the involvement of the *tonB1* operon genes (*tonB1-exbB1-exbD1-exbD2*) in the uptake of lignin-derived aromatic compounds, each plasmid carrying *tonB1* (pJB-tonB1), *tonB1*-

Substrate	WT + pJB861	WT + pJB-tonB1	WT + pJB-t1-D1	WT + pJB-t1-D12
DDVA	7.0 ± 1.1	12 ± 0.6** [1.8]	15 ± 0.1*** [2.2]	18 ± 1.4*** [2.6]
GGE	45 ± 2.4	49 ± 1.7	53 ± 1.1* [1.2]	53 ± 0.2** [1.2]
PR	35 ± 1.2	36 ± 0.8	43 ± 0.7** [1.2]	43 ± 2.2* [1.2]
DCA	133 ± 3.4	142 ± 7.4	164 ± 1.8*** [1.2]	161 ± 0.5*** [1.2]
HMPPD	98 ± 4.6	101 ± 5.8	81 ± 13	111 ± 4.2* [1.1]
AV	42 ± 4.4	41 ± 1.1	42 ± 2.6	41 ± 1.0
FA	73 ± 2.3	74 ± 1.3	74 ± 2.8	86 ± 1.0** [1.2]
VN	229 ± 13	257 ± 15	187 ± 35	229 ± 8.0
VA	38 ± 2.9	38 ± 1.9	42 ± 1.3	47 ± 0.5* [1.2]
SN	210 ± 16	197 ± 20	212 ± 16	193 ± 8.6
SA	44 ± 4.0	44 ± 2.0	51 ± 1.7	59 ± 1.8** [1.4]
PCA	73 ± 1.8	72 ± 2.9	75 ± 1.3	85 ± 2.2** [1.2]

Table 2. The conversion rates of lignin-derived aromatic compounds by SYK-6 cells overexpressing the *tonB1* operon genes. The conversion rates were calculated from the results of Fig. S8 using the decreasing amount of each substrate at the time interval (DDVA, 0–5.0 h; GGE, 0–1.5 h; PR, 0–2.0 h; DCA, 0–0.5 h; HMPPD, 0–0.5 h; AV, 0–2.0 h; FA, 0–1.0 h; VN, 0–0.5 h; VA, 0–2.0 h; SN, 0–0.5 h; SA, 0–1.5 h; PCA, 0–1.0 h), where almost linear conversions of the substrates were observed. Each value is the average ± the standard deviation of three independent experiments. * $P < 0.05$, ** $P < 0.01$, *** $P < 0.001$ (values indicating significance between the conversion rates of SYK-6 cells harboring pJB861 and SYK-6 cells harboring pJB-tonB1, pJB-t1-D1, or pJB-t1-D12 from unpaired, two-tailed *t*-test). The *P* value of each field without an asterisk, $P > 0.05$. Values in the brackets indicate fold change between the conversion rates by SYK-6 cells harboring pJB861 and SYK-6 cells harboring pJB-tonB1, pJB-t1-D1, or pJB-t1-D12.

exbB1-exbD1 (pJB-t1-D1), and *tonB1-exbB1-exbD1-exbD2* (pJB-t1-D12) was introduced into SYK-6 cells. We measured the capacity of resting cells of SYK-6 harboring pJB-tonB1, pJB-t1-D1, or pJB-t1-D12 to convert DDVA, GGE, PR, DCA, HMPPD, AV, FA, VN, VA, SN, SA, and PCA. The introduction of pJB-tonB1 increased only the conversion rate of DDVA by ca. 1.8-fold, while the introduction of pJB-t1-D1 or pJB-t1-D12 increased the conversion rate of DDVA, GGE, PR, DCA, HMPPD, FA, VA, SA, and PCA by ca. 1.1–2.6-fold (Table 2, Figs. S8, S9). However, the introduction of these plasmids did not promote the growth of SYK-6 on DDVA, FA, VN, VA, PCA, and SEMP (Fig. S10). On the other hand, the conversion rates of AV, VN, and SN by SYK-6 cells harboring pJB-tonB1, pJB-t1-D1, or pJB-t1-D12 were comparable to those of the control strain. AV, VN, and SN are presumed to be taken up by the outer membrane transporters other than TBBDT or diffused without transporters.

To determine whether the enhanced conversion capacity of the strains that overexpress the *tonB1* operon genes was due to their increased uptake capacity, we assessed the DDVA uptake of these strains using a previously constructed DDVA biosensor^{9,24}. Consequently, overexpression of *tonB1*, *tonB1-exbB1-exbD1*, and *tonB1-exbB1-exbD1-exbD2* increased the DDVA uptake capacity ca. 1.4-, 1.3-, and 1.6-fold, respectively, compared to the control strain (Fig. 4). These results strongly suggest that the *tonB1* operon genes are involved in the uptake of DDVA. Similarly, strains overexpressing the *tonB1* operon genes likely enhanced the conversion of GGE, PR, DCA, HMPPD, FA, VA, SA, and PCA due to the enhanced capacity to take up each substrate. Therefore, these lignin-derived aromatic compounds seem to be taken up by TBBDTs.

We investigated the cellular localization of TonB1. Western blot analysis using anti-TonB1 antibodies against a cell extract and a total membrane fraction obtained from SYK-6 cells grown in LB showed a clear signal in a total membrane fraction, indicating that TonB1 is localized in the cell membrane (Fig. S11).

Sphingomonadaceae, to which SYK-6 belongs, contains many strains capable of degrading recalcitrant aromatic compounds such as lignin-derived aromatic compounds and polycyclic aromatic hydrocarbons²⁵. These strains have as many or more TBBDT and Ton complex genes as SYK-6^{25,27}. Therefore, we examined whether the *tonB1* operon genes of SYK-6 are conserved in the Sphingomonadaceae strains listed in Table S1. These strains have genes showing 43–58% amino acid sequence identity with *tonB1*, 35–81% with *exbB1*, 35–81% with *exbD1*, and 55–75% with *exbD2*. Additionally, these genes have a similar gene organization as the SYK-6 *tonB1* operon (Fig. S12). Based on these facts, it is highly likely that the *tonB1* operon-like genes play a central role in TonB-dependent uptake in these Sphingomonadaceae.

ExbB2/TolQ and ExbD3/TolR constitute the Tol-Pal system. Since mutations in genes constituting the Tol-Pal system have been reported to cause reduced resistance to detergents²⁸, we compared the growth of wild type, $\Delta exbB2/tolQ$, and $\Delta exbD3/tolR$ in LB with or without 0.3 mg/ml sodium deoxycholate (NaDOC) or 0.05 mg/ml sodium dodecyl sulfate (SDS) (Fig. 5). The addition of NaDOC or SDS to the wild type had little effect on growth; however, the growth of $\Delta exbB2/tolQ$ and $\Delta exbD3/tolR$ was significantly reduced in the presence of the detergents.

Mutations in the Tol-Pal system genes cause instability of the outer membrane structure, resulting in the secretion of the outer membrane vesicles (OMVs)³². Therefore, we observed the cell surface structure of the

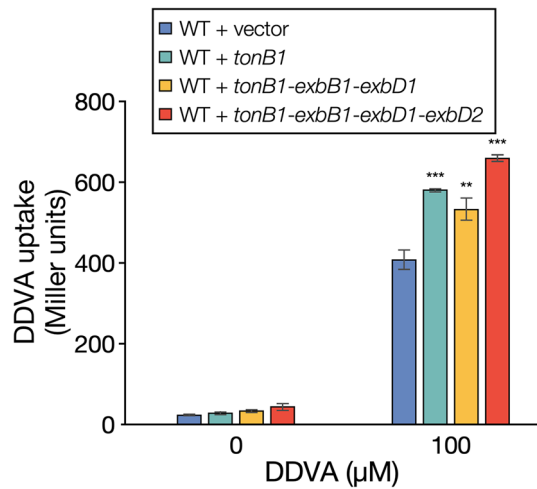


Figure 4. DDVA uptake by SYK-6 cells overexpressing the *tonB1* operon genes. The uptake of DDVA by SYK-6 cells overexpressing the *tonB1* operon genes was evaluated using the DDVA sensor plasmid pS-XR, which was constructed by applying the regulatory system of the DDVA catabolic genes²⁴. The β -galactosidase activities of cells of SYK-6(pS-XR + pSEVA338 [vector]), SYK-6(pS-XR + pS-*tonB1*), SYK-6(pS-XR + pS-t1-D1), and SYK-6(pS-XR + pS-t1-D12) incubated in Wx-SEMP with or without 100 μ M DDVA were measured. Each value is the average \pm the standard deviation of three independent experiments. Asterisks show statistically significant differences between cells overexpressing the *tonB1* operon genes and vector control cells incubated in the presence of 100 μ M DDVA. **, $P < 0.01$, ***, $P < 0.001$ (unpaired, two-tailed *t*-test). This figure was generated using Canvas X Draw version 7.0.2. (<https://www.canvasgfx.com/products/canvas-x-draw>).

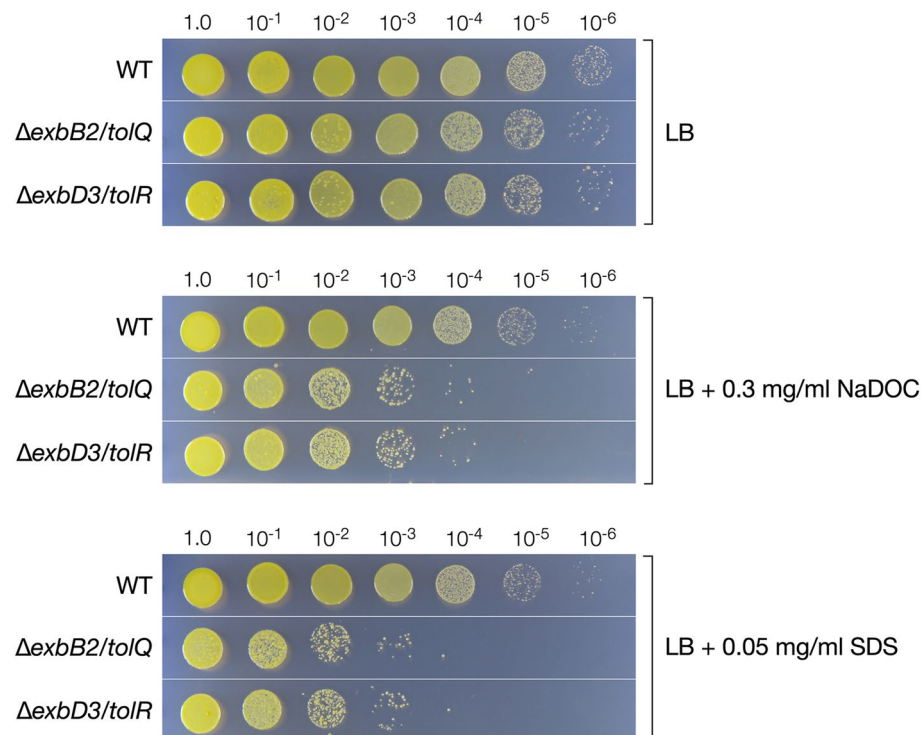


Figure 5. Δ *exbB2/tolQ* and Δ *exbD3/tolR* cells show susceptibility to detergents. The cells of SYK-6, Δ *exbB2/tolQ*, and Δ *exbD3/tolR* were grown in LB with or without 0.3 mg ml⁻¹ of NaDOC or 0.05 mg ml⁻¹ SDS. The cell diluted with Wx buffer (10 μ l) were dropped onto LB agar medium and incubated at 30 $^{\circ}$ C for 72 h. This figure was generated using Canvas X Draw version 7.0.2. (<https://www.canvasgfx.com/products/canvas-x-draw>).

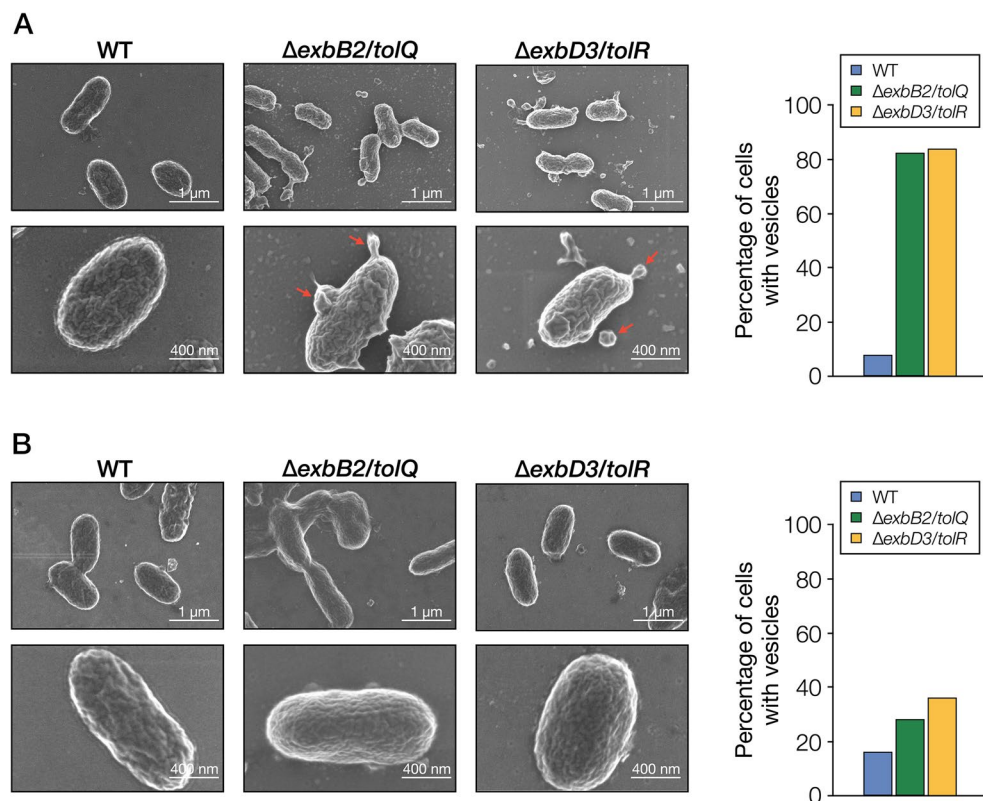


Figure 6. SEM analysis of SYK-6, $\Delta exbB2/tolQ$, and $\Delta exbD3/tolR$. **(A)** FE-SEM images of SYK-6, $\Delta exbB2/tolQ$, and $\Delta exbD3/tolR$ cells grown in LB. Red arrows indicate blebbing vesicles. **(B)** FE-SEM images of SYK-6, $\Delta exbB2/tolQ$, and $\Delta exbD3/tolR$ cells grown in LB with 5 mM FA. The right figure shows the percentage of cells with vesicles. Outer membrane vesiculation was quantified by imaging 50 bacterial cells and expressed as the percentage of cells with OMV. This figure was generated using Canvas X Draw version 7.0.2. (<https://www.canva.com/products/canvas-x-draw>).

wild type, $\Delta exbB2/tolQ$, and $\Delta exbD3/tolR$ grown in LB using field emission scanning electron microscopy (FE-SEM) (Fig. 6A). The formation of blebs was observed on the cell surface of $\Delta exbB2/tolQ$ and $\Delta exbD3/tolR$. To examine whether OMVs were secreted into the culture medium of $\Delta exbB2/tolQ$ and $\Delta exbD3/tolR$, we performed western blot analysis using anti-DdvT antibodies against the culture supernatants of wild type, $\Delta exbB2/tolQ$, and $\Delta exbD3/tolR$ grown in LB since OMVs are thought to contain outer membrane proteins (Figs. 7, S13)^{24,32}. DdvT was detected in the culture supernatants of $\Delta exbB2/tolQ$ and $\Delta exbD3/tolR$, but not in the culture supernatant of the wild type. Furthermore, DdvT was not detected in the ultracentrifuged supernatant obtained from the cultures of $\Delta exbB2/tolQ$ and $\Delta exbD3/tolR$, suggesting the presence of outer membrane fractions in their culture supernatants. Western blot analysis using anti-TonB1 antibodies as an inner membrane marker protein showed that TonB1 was detected only in cell extracts of all strains. These results indicate that OMVs are present in the culture supernatants of $\Delta exbB2/tolQ$ and $\Delta exbD3/tolR$.

FA was the only carbon source that did not reduce the growth of $\Delta exbB2/tolQ$ and $\Delta exbD3/tolR$ (Fig. 3). Thus, vesiculation of these mutants during FA catabolism was evaluated. Interestingly, DdvT was not detected in the culture supernatants of $\Delta exbB2/tolQ$ and $\Delta exbD3/tolR$ grown in LB containing 5 mM FA (Fig. 7). When $\Delta exbB2/tolQ$ and $\Delta exbD3/tolR$ were grown in LB containing 5 mM PCA, a catabolite of FA (Fig. S14A), DdvT was detected in their culture supernatants, suggesting that the outer membrane structure of $\Delta exbB2/tolQ$ and $\Delta exbD3/tolR$ was specifically stabilized during FA catabolism. The observation of the cell surface structure of $\Delta exbB2/tolQ$ and $\Delta exbD3/tolR$ grown in LB containing 5 mM FA showed that the formation of blebs was significantly suppressed during FA catabolism (Fig. 6B). In SYK-6 cells, FA is converted to VN through the addition of coenzyme A (CoA) to the C γ position and the subsequent release of acetyl-CoA (Fig. S14A)³⁵. To get insight into why the growth capacity of $\Delta exbB2/tolQ$ and $\Delta exbD3/tolR$ was not reduced when FA was used as a carbon source (Fig. 3), we constructed a double mutant of $exbD3/tolR$ and the PDC hydrolase gene *ligI* ($\Delta exbD3/tolR$ *ligI*) (Figs. S4, S14A). This strain produces acetyl-CoA during FA catabolism, but the conversion of VN from FA stops at the PDC. Growth measurement of $\Delta exbD3/tolR$ *ligI* in the presence or absence of FA showed that the addition of more than 1 mM FA compensated for the growth in diluted LB (Fig. S14B). In contrast, the addition of VA and PCA did not positively affect the growth of $\Delta exbD3/tolR$ *ligI* in diluted LB. Based on these results, the continuous supply of acetyl-CoA produced in the second step of FA catabolism to fatty acid biosynthesis may reduce the damage to the outer membrane caused by the disruption of *exbB2/tolQ* and *exbD3/tolR* (Fig. S14A). However, further investigation is needed to elucidate the actual mechanism.

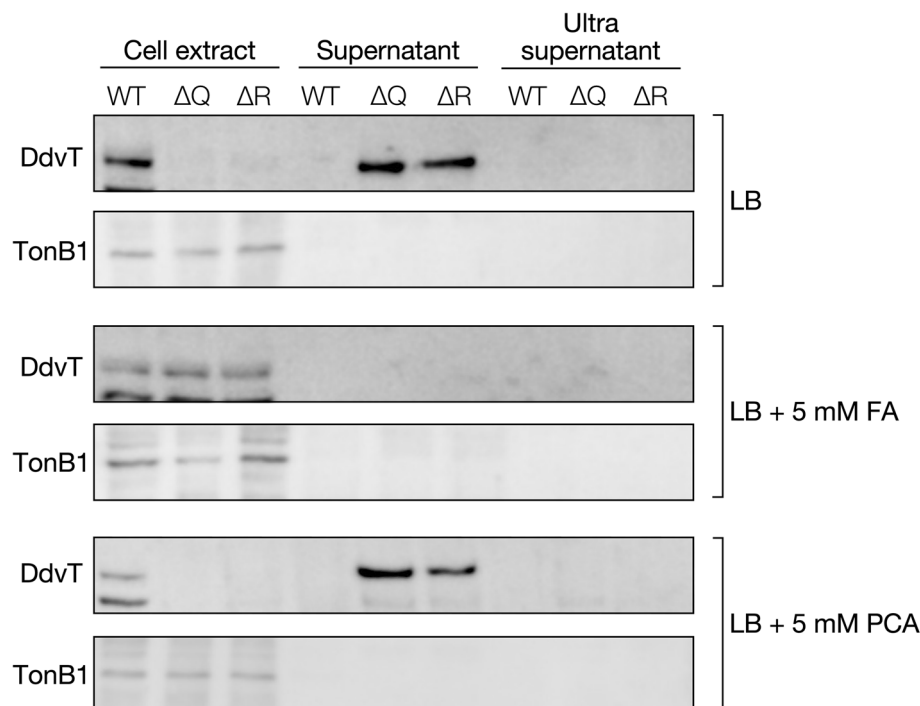


Figure 7. Detection of the outer membrane fraction in the culture supernatants of *exbB2/tolQ* and *exbD3/tolR* mutants. Cells of the wild type (WT), $\Delta exbB2/tolQ$ (ΔQ), and $\Delta exbD3/tolR$ (ΔR) were grown in LB with or without 5 mM FA or PCA. As shown in Fig. S13, after centrifugation, the supernatants of the cultures were collected (supernatant), and the cell extracts were prepared. The supernatants were further ultracentrifuged, and the resulting supernatants were collected (ultrasupernatant). Western blot analysis using anti-DdvT and anti-TonB1 antibodies was performed against cell extracts (10 μ g of protein), 20 μ l of the supernatant, and 20 μ l of the ultrasupernatant. The uncropped blot images are shown in Fig. S16. This figure was generated using Canvas X Draw version 7.0.2. (<https://www.canvasgxf.com/products/canvas-x-draw>).

In the Sphingomonadaceae strains that can degrade aromatic compounds listed in Table S2, genes with high similarity amino acid sequences (*exbB2/tolQ*, 56–63% identity; *exbD3/tolR*, 46–62% identity; *tolA*, 33–52% identity; *tolB*, 58–73% identity; *pal*, 57–70% identity) and gene organization with the Tol-Pal system genes of SYK-6 were conserved (Fig. S15). This high degree of conservation suggests that these genes play similar roles to the corresponding SYK-6 genes in these bacterial strains.

Conclusions

Overexpression of the *tonB1* operon genes in SYK-6 enhanced the capacity to convert at least five lignin-derived dimers and four monomers. These results strongly suggest that TBDTs mediate the uptake of these lignin-derived aromatic compounds, and the Ton complex composed of TonB1–ExbB1–ExbD1–ExbD2 is involved in their uptake (Fig. 8). Besides, *exbB2/tolQ* and *exbD3/tolR* constitute the Tol-Pal system stabilizing the outer membrane structure. Based on this study's results, it is expected that microbial conversion systems with enhanced uptake capacity will be developed through the identification of TBDT genes involved in the outer membrane transport of each lignin-derived aromatic compound.

Methods

Bacterial strains, plasmids, culture conditions, and substrates. The strains and plasmids used in this study are listed in Table S3. *Sphingobium* sp. SYK-6 (NBRC 103272/JCM 17495) and its mutants were grown at 30 °C with shaking (160 rpm) in LB or Wx minimal medium with SEMP³⁴. Media for SYK-6 transformants and mutants were supplemented with 50 mg l⁻¹ kanamycin (Km) or 30 mg l⁻¹ chloramphenicol (Cm). *E. coli* strains were cultured in LB at 37 °C. Media for *E. coli* transformants carrying antibiotic resistance markers were supplemented with 25 mg l⁻¹ Km or 30 mg l⁻¹ Cm. Lignin-derived compounds were purchased from Sigma-Aldrich and Tokyo Chemical Industry Co., Ltd. DDVA, PR, DCA, and HMPPD were synthesized as previously described^{35–38}.

Mutant construction. Plasmids for gene disruption were constructed by amplifying ca. 1-kb fragments carrying upstream and downstream regions of each gene by PCR with SYK-6 genome DNA as a template and the primer pairs (Table S4). The resultant PCR fragments were inserted into the BamHI site in pAK405 by NEBuilder HiFi DNA assembly cloning kit (New England Biolabs, Inc.). These plasmids were independently

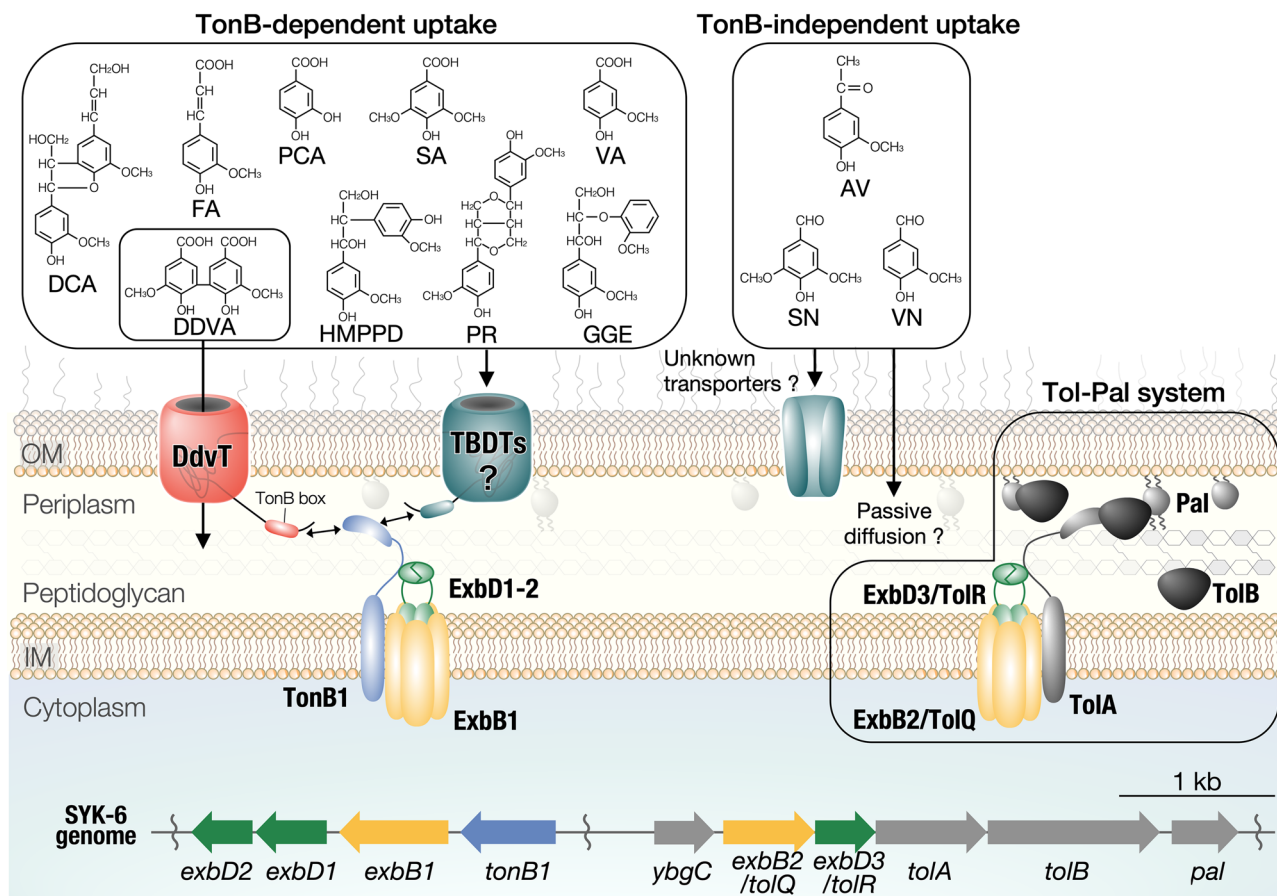


Figure 8. Proposed outer membrane transport of lignin-derived aromatic compounds in SYK-6. Outer membrane transport of GGE, PR, DCA, HMPPD, FA, VA, SA, and PCA is thought to be mediated by TBDTs, and the involvement of TonB1–ExbB1–ExbD1–ExbD2 as the Ton complex is strongly suggested. AV, VN, and SN are presumed to be taken up by transporters other than TBDT or passive diffusion. ExbB2/TolQ and ExbD3/TolR are the components of the Tol–Pal system that stabilizes the outer membrane structure. OM, outer membrane; IM, inner membrane. This figure was generated using Canvas X Draw version 7.0.2. (<https://www.canvasgfx.com/products/canvas-x-draw>).

introduced into SYK-6 and its mutant cells by triparental mating, and candidate mutants were isolated as previously described³⁹. The disruption of the genes was confirmed by colony PCR using primer pairs (Table S4). The plasmids for gene complementation and overexpression (Table S3) were introduced into SYK-6 and the mutant cells by electroporation.

Sequence analysis. DNA sequencing of PCR amplification products was conducted by Eurofins Genomics. Sequence analysis was conducted using the MacVector program v.15.5.2. Additionally, sequence similarity searches, multiple alignments, and pairwise alignments were conducted using the BLAST⁴⁰, Clustal Omega⁴¹, and EMBOSS programs⁴², respectively.

Growth measurement. Cells of SYK-6, its mutants, and complemented strains were grown in LB for 24 h. The cells were harvested by centrifugation at $4,800 \times g$ for 5 min, washed twice with Wx buffer, and resuspended in 3 ml of the same buffer. The cells were then inoculated into diluted LB, Wx medium containing SEMP, or Wx medium containing 5 mM DDVA, FA, VN, VA, SA, or PCA to an OD_{660} of 0.2. Since SYK-6 exhibits auxotrophy for methionine when grown in a methoxy-group-free substrate, 0.13 mM methionine was added to the medium to grow on PCA. Cells were incubated at 30 °C with shaking (60 rpm), and cell growth was monitored every hour by measuring the OD_{660} with a TVS062CA biophotorecorder (Advantec Co., Ltd.). For the assay of complemented strains, Km and 1 mM *m*-toluate (an inducer of the P_m promoter in pJB861) were added to the medium; for the assay of SYK-6 cells overexpressing the *tonB1* operon genes, Km and 0.5 mM *m*-toluate were added to the medium.

Resting cell assay. Cells of SYK-6 and its mutants were grown in LB for 20 h and harvested by centrifugation at $14,100 \times g$ for 5 min. The cells were washed twice with 50 mM Tris-HCl buffer (pH 7.5) and resuspended in 1 ml of the same buffer. For conversion of AV, cells were grown in Wx-SEMP until OD_{660} reached 0.5 and

then incubated in the presence of 5 mM AV for 12 h. The cells were then incubated in 50 mM Tris-HCl buffer (pH 7.5) with 100 μ M DDVA (OD_{600} of the cells, 5.0; reaction time, 6 h), 200 μ M GGE (5.0; 6 h), 100 μ M PR (0.5; 3 h), 100 μ M DCA (0.5; 2 h), 100 μ M HMPPD (2.0; 2 h), 100 μ M AV (0.5; 3 h), 100 μ M FA (1.0; 2 h), 200 μ M VN (0.2; 1 h), 100 μ M VA (2.0; 2 h), 200 μ M SN (0.4; 1 h), 100 μ M SA (2.0; 2 h), or 100 μ M PCA (2.0; 1 h). Samples were collected periodically, and the reactions were stopped by centrifugation at $18,800 \times g$ for 10 min. The supernatants were diluted fivefold in water, filtered, and analyzed using high-performance liquid chromatography (HPLC). For the analysis of SYK-6 cells harboring plasmids carrying the *tonB1* operon genes, the cells grown in LB containing Km and 0.5 mM *m*-toluate were employed. These cells were incubated with lignin-derived aromatic compounds under the conditions described above, with the following exceptions. For the conversion of 100 μ M DDVA, 100 μ M GGE, 100 μ M PR, and 100 μ M PCA, cells with OD_{600} of 5.0, 3.0, 0.2, and 1.0, respectively, were used and incubated with each substrate for 5, 3, 4, and 2 h.

HPLC conditions. HPLC analysis was conducted using an Acquity UPLC system (Waters Corporation) with a TSKgel ODS-140HTP column (2.1 by 100 mm; Tosoh Corporation). All analyses were conducted at a flow rate of 0.5 ml min⁻¹. The mobile phase was a mixture of solution A (acetonitrile containing 0.1% formic acid) and solution B (water containing 0.1% formic acid) under the following conditions: i) conversion of DDVA, 0–2.5 min, 15% A; ii) conversion of GGE, 0–3.2 min, linear gradient from 5 to 40% A; 3.2–6.0 min, decreasing gradient from 40 to 5% A; 6.0–7.0 min, 5% A. iii) conversion of PR, 0–5.0 min, 20% A. iv) conversion of DCA, 0–2.0 min, 25% A. v) conversion of HMPPD, 0–2.0 min, 10% A. vi) conversion of AV, 0–2.0 min, 15% A. vii) conversion of FA, 0–2.5 min, 15% A. viii) conversion of VN and SN, 0–2.0 min, 15% A. ix) conversion of VA and SA, 0–2.0 min, 10% A. x) conversion of PCA, 0–2.0 min, 10% A. DDVA, GGE, PR, DCA, HMPPD, AV, FA, VN, VA, SN, SA, and PCA were detected at 265, 270, 280, 277, 278, 276, 322, 280, 260, 308, 275, and 260 nm, respectively. Peaks were quantified based on the standard curves prepared with authentic compounds.

DDVA uptake assay. Cells of SYK-6 harboring pS-XR and pS-tonB1, pS-t1-D1, or pS-t1-D12 grown in LB containing Km and Cm for 20 h were harvested by centrifugation at $4,800 \times g$ for 5 min, washed twice with Wx buffer, and resuspended in 1 ml Wx-SEMP. The cells were then inoculated into Wx-SEMP containing 0.5 mM *m*-toluate with or without 100 μ M DDVA to an OD_{600} of 2.0. Samples were incubated at 30 °C with shaking (1,500 rpm) for 3 h. The β -galactosidase activity of the cells was measured using 2-nitrophenyl- β -D-galactopyranoside as the substrate, according to a modified Miller assay [[https://openwetware.org/wiki/Beta-Galactosidase_Assay_\(A_better_Miller\)](https://openwetware.org/wiki/Beta-Galactosidase_Assay_(A_better_Miller))]⁹. β -galactosidase activity was expressed as Miller units.

Detergent resistance assay. Cells of SYK-6 and its mutants were grown in LB for 20 h were harvested by centrifugation at $4,800 \times g$ for 5 min and resuspended in Wx buffer. The cells were inoculated into LB with or without 0.05 mg ml⁻¹ SDS or 0.3 mg ml⁻¹ NaDOC to an OD_{600} of 0.2 and incubated at 30 °C for 24 h. The cultured cells were then serially diluted with Wx buffer, and 10 μ l of each cell suspension was dropped onto an LB plate. The plates were incubated at 30 °C for 72 h.

Western blot analysis. A peptide corresponding to residues 199–210 (QAGNPIRTKDRR) of TonB1 was synthesized and used as an antigen to obtain antisera for TonB1 in rabbits (Cosmo Bio, Inc.). Anti-TonB1-peptide antibodies were obtained by purifying the antiserum using peptide affinity column chromatography (Cosmo Bio, Inc.). Anti-DdvT antibodies were obtained in a previous study²⁴. Total membrane fractions were prepared as described previously from SYK-6 cells incubated in LB for 20 h²⁴. TonB1 and DdvT were detected by western blot analysis using anti-TonB1 antibodies (0.11 μ g ml⁻¹) and anti-DdvT antibodies (0.25 μ g ml⁻¹) as described previously²⁴. Horseradish peroxidase-conjugated goat anti-rabbit IgG antibodies (Invitrogen, 0.2 μ g ml⁻¹) were used as the secondary antibodies. Protein concentrations were determined by the Bradford method using a Bio-Rad protein assay kit or Lowry's assay with a DC protein assay kit (Bio-Rad Laboratories). TonB1 and DdvT were detected using the ECL Western Blotting Detection System (GE Healthcare) with a LumiVision PRO image analyzer (Aisin Seiki Co., Ltd).

Detection of outer membrane vesiculation of Δ exbB2/*tolQ* and Δ exbD3/*tolR*. Cells of SYK-6 and its mutants were grown in LB with or without 5 mM FA or PCA for 20 h were harvested by centrifugation at $19,000 \times g$ for 10 min. The supernatant of the centrifuged culture was filtered with a 0.45 μ m membrane filter (supernatant fraction). Then, the supernatant fraction was ultracentrifuged at $120,000 \times g$ for 60 min to obtain ultracentrifuged supernatant (ultrasupernatant fraction). The cells were washed twice with 50 mM Tris-HCl buffer (pH 7.5) containing 150 mM NaCl and resuspended in the same buffer containing 1 mM phenylmethylsulfonyl fluoride. The cells were disrupted by sonication, and cell lysate was obtained. Each fraction was separated by SDS-7.5% or 15% polyacrylamide gel electrophoresis and performed western blot analysis using anti-TonB1 antibodies and anti-DdvT antibodies as described above.

FE-SEM analysis. Cells of SYK-6 and its mutants grown on LB plates with or without 5 mM FA for 48 h were deposited on poly-D-lysine coated glass (Cosmo Bio, Inc.) and fixed with 2.0% glutaraldehyde solution in 200 mM sodium phosphate buffer (pH 7.5) for 2 h at room temperature. Fixed cells were washed twice with the same buffer and dehydrated in an ethanol gradient of 25%, 50%, 75%, 90%, and 100% for 15 min per step. Samples were dried using an evaporator for 8 h at 30 °C and sputter-coated with Os. Cell images were obtained using a HITACHI SU8230 field emission SEM with a beam accelerating voltage of 1.0 kV.

Statistics and reproducibility. All results were obtained from $n = 3$ independent experiments. Statistical tests were performed using GraphPad Prism9 (GraphPad software). Unpaired, two-tailed t -test were used as shown in figure legends. $P < 0.05$ was considered statistically significant.

Data availability

All data supporting this study are available within the article and its Supplementary Information or are available from the corresponding author upon request.

Received: 16 August 2021; Accepted: 27 October 2021

Published online: 17 November 2021

References

1. Vanholme, R., Demedts, B., Morreel, K., Ralph, J. & Boerjan, W. Lignin biosynthesis and structure. *Plant Physiol.* **153**, 895–905. <https://doi.org/10.1104/pp.110.155119> (2010).
2. Calvo-Flores, F. G. & Dobado, J. A. Lignin as renewable raw material. *ChemSuschem* **3**, 1227–1235. <https://doi.org/10.1002/cssc.201000157> (2010).
3. Beckham, G. T., Johnson, C. W., Karp, E. M., Salvachúa, D. & Vardon, D. R. Opportunities and challenges in biological lignin valorization. *Curr. Opin. Biotechnol.* **42**, 40–53. <https://doi.org/10.1016/j.copbio.2016.02.030> (2016).
4. Kamimura, N. *et al.* Bacterial catabolism of lignin-derived aromatics: New findings in a recent decade: Update on bacterial lignin catabolism. *Environ. Microbiol. Rep.* **9**, 679–705. <https://doi.org/10.1111/1758-2229.12597> (2017).
5. Masai, E., Katayama, Y. & Fukuda, M. Genetic and biochemical investigations on bacterial catabolic pathways for lignin-derived aromatic compounds. *Biosci. Biotechnol. Biochem.* **71**, 1–15. <https://doi.org/10.1271/bbb.60437> (2007).
6. Otsuka, Y. *et al.* Efficient production of 2-pyrone 4,6-dicarboxylic acid as a novel polymer-based material from protocatechuate by microbial function. *Appl. Microbiol. Biotechnol.* **71**, 608–614. <https://doi.org/10.1007/s00253-005-0203-7> (2006).
7. Higuchi, Y. *et al.* Discovery of novel enzyme genes involved in the conversion of an arylglycerol- β -ether metabolite and their use in generating a metabolic pathway for lignin valorization. *Metab. Eng.* **55**, 258–267. <https://doi.org/10.1016/j.ymben.2019.08.002> (2019).
8. Mori, K., Kamimura, N. & Masai, E. Identification of the protocatechuate transporter gene in *Sphingobium* sp. strain SYK-6 and effects of overexpression on production of a value-added metabolite. *Appl. Microbiol. Biotechnol.* **102**, 4807–4816. <https://doi.org/10.1007/s00253-018-8988-3> (2018).
9. Mori, K., Niinuma, K., Fujita, M., Kamimura, N. & Masai, E. DdvK, a novel major facilitator superfamily transporter essential for 5,5'-dehydrodivanillate uptake by *Sphingobium* sp. strain SYK-6. *Appl. Environ. Microbiol.* **84**, e01314–18. <https://doi.org/10.1128/AEM.01314-18> (2018).
10. Nikaido, H. Molecular basis of bacterial outer membrane permeability revisited. *Microbiol. Mol. Biol. Rev.* **67**, 593–656. <https://doi.org/10.1128/mmb.67.4.593-656.2003> (2003).
11. Josts, I., Veith, K. & Tidow, H. Ternary structure of the outer membrane transporter FoxA with resolved signalling domain provides insights into TonB-mediated siderophore uptake. *Elife* **8**, e48528. <https://doi.org/10.7554/eLife.48528> (2019).
12. Shultis, D. D., Purdy, M. D., Banchs, C. N. & Wiener, M. C. Outer membrane active transport: structure of the BtuB:TonB complex. *Science* **312**, 1396–1399. <https://doi.org/10.1126/science.1127694> (2006).
13. Ratliff, A. C., Buchanan, S. K. & Celia, H. Ton motor complexes. *Curr. Opin. Struct. Biol.* **67**, 95–100. <https://doi.org/10.1016/j.sbi.2020.09.014> (2021).
14. Chu, B. C., Peacock, R. S. & Vogel, H. J. Bioinformatic analysis of the TonB protein family. *Biomaterials* **20**, 467–483. <https://doi.org/10.1007/s10534-006-9049-4> (2007).
15. Blanvillain, S. *et al.* Plant carbohydrate scavenging through TonB-dependent receptors: A feature shared by phytopathogenic and aquatic bacteria. *PLoS ONE* **2**, e224. <https://doi.org/10.1371/journal.pone.0000224> (2007).
16. Bolam, D. N. & van den Berg, B. TonB-dependent transport by the gut microbiota: Novel aspects of an old problem. *Curr. Opin. Struct. Biol.* **51**, 35–43. <https://doi.org/10.1016/j.sbi.2018.03.001> (2018).
17. Calmettes, C. *et al.* The molecular mechanism of zinc acquisition by the neisserial outer-membrane transporter ZnuD. *Nat. Commun.* **6**, 7996. <https://doi.org/10.1038/ncomms8996> (2015).
18. Madej, M. *et al.* Structural and functional insights into oligopeptide acquisition by the RagAB transporter from *Porphyromonas gingivalis*. *Nat. Microbiol.* **5**, 1016–1025. <https://doi.org/10.1038/s41564-020-0716-y> (2020).
19. Szczepaniak, J., Press, C. & Kleantous, C. The multifarious roles of Tol-Pal in Gram-negative bacteria. *FEMS Microbiol. Rev.* **44**, 490–506. <https://doi.org/10.1093/femsre/fuaa018> (2020).
20. Braun, V. & Herrmann, C. Evolutionary relationship of uptake systems for biopolymers in *Escherichia coli*: Cross-complementation between the TonB-ExbB-ExbD and the TolA-TolQ-TolR proteins. *Mol. Microbiol.* **8**, 261–268. <https://doi.org/10.1111/j.1365-2958.1993.tb01570.x> (1993).
21. Neher, T. M. & Lueking, D. R. *Pseudomonas fluorescens ompW*: plasmid localization and requirement for naphthalene uptake. *Can. J. Microbiol.* **55**, 553–563. <https://doi.org/10.1139/w09-002> (2009).
22. Tamber, S., Ochs, M. M. & Hancock, R. E. Role of the novel OprD family of porins in nutrient uptake in *Pseudomonas aeruginosa*. *J. Bacteriol.* **188**, 45–54. <https://doi.org/10.1128/JB.188.1.45-54.2006> (2006).
23. Hong, H., Patel, D. R., Tamm, L. K. & van den Berg, B. The outer membrane orotein OmpW forms an eight-stranded β -barrel with a hydrophobic channel. *J. Biol. Chem.* **281**, 7568–7577. <https://doi.org/10.1074/jbc.M512365200> (2006).
24. Fujita, M. *et al.* A TonB-dependent receptor constitutes the outer membrane transport system for a lignin-derived aromatic compound. *Commun. Biol.* **2**, 432. <https://doi.org/10.1038/s42003-019-0676-z> (2019).
25. Samantarrai, D., Lakshman Sagar, A., Gudla, R. & Siddavattam, D. TonB-dependent transporters in Sphingomonads: Unraveling their distribution and function in environmental adaptation. *Microorganisms* **8**, 359. <https://doi.org/10.3390/microorganisms8030359> (2020).
26. Liang, J. *et al.* Benzo[a]pyrene might be transported by a TonB-dependent transporter in *Novosphingobium pentaromativorans* US6-1. *J. Hazard. Mater.* **404**, 124037. <https://doi.org/10.1016/j.jhazmat.2020.124037> (2021).
27. Fujita, M. *et al.* Iron acquisition system of *Sphingobium* sp. strain SYK-6, a degrader of lignin-derived aromatic compounds. *Sci. Rep.* **10**, 12177. <https://doi.org/10.1038/s41598-020-68984-2> (2020).
28. Szczepaniak, J. *et al.* The lipoprotein Pal stabilises the bacterial outer membrane during constriction by a mobilisation-and-capture mechanism. *Nat. Commun.* **11**, 1305. <https://doi.org/10.1038/s41467-020-15083-5> (2020).
29. Gao, T., Meng, Q. & Gao, H. Thioesterase YbgC affects motility by modulating c-di-GMP levels in *Shewanella oneidensis*. *Sci. Rep.* **7**, 3932. <https://doi.org/10.1038/s41598-017-04285-5> (2017).
30. Baker, K. R. & Postle, K. Mutations in *Escherichia coli* ExbB transmembrane domains identify scaffolding and signal transduction functions and exclude participation in a proton pathway. *J. Bacteriol.* **195**, 2898–2911. <https://doi.org/10.1128/jb.00017-13> (2013).

31. Celia, H. *et al.* Structural insight into the role of the Ton complex in energy transduction. *Nature* **538**, 60–65. <https://doi.org/10.1038/nature19757> (2016).
32. Bernadac, A., Gavioli, M., Lazzaroni, J.-C., Raina, S. & Lloubès, R. *Escherichia coli tol-pal* mutants form outer membrane vesicles. *J. Bacteriol* **180**, 4872–4878. <https://doi.org/10.1128/JB.180.18.4872-4878.1998> (1998).
33. Masai, E. *et al.* Cloning and characterization of the ferulic acid catabolic genes of *Sphingomonas paucimobilis* SYK-6. *Appl. Environ. Microbiol.* **68**, 4416–4424. <https://doi.org/10.1128/aem.68.9.4416-4424.2002> (2002).
34. Kasai, D. *et al.* Characterization of FerC, a MarR-type transcriptional regulator, involved in transcriptional regulation of the ferulate catabolic operon in *Sphingobium* sp. strain SYK-6. *FEMS Microbiol. Lett.* **332**, 68–75. <https://doi.org/10.1111/j.1574-6968.2012.02576.x> (2012).
35. Peng, X. *et al.* Cloning of a *Sphingomonas paucimobilis* SYK-6 gene encoding a novel oxygenase that cleaves lignin-related biphenyl and characterization of the enzyme. *Appl. Environ. Microbiol.* **64**, 2520–2527. <https://doi.org/10.1128/AEM.64.7.2520-2527.1998> (1998).
36. Fukuhara, Y. *et al.* Discovery of pinoresinol reductase genes in Sphingomonads. *Enzyme Microb. Technol.* **52**, 38–43. <https://doi.org/10.1016/j.enzmictec.2012.10.004> (2013).
37. Takahashi, K. *et al.* Characterization of the catabolic pathway for a phenylcoumaran-type lignin-derived biaryl in *Sphingobium* sp. strain SYK-6. *Biodegradation* **25**, 735–745. <https://doi.org/10.1007/s10532-014-9695-0> (2014).
38. Nakatsubo, F. & Higuchi, T. Synthesis of 1,2-diarylpropane-1,3-diols and determination of their configurations. *Holzforschung* **29**, 193–198. <https://doi.org/10.1515/hfsg.1975.29.6.193> (1975).
39. Kaczmarczyk, A., Vorholt, J. A. & Francez-Charlot, A. Markerless gene deletion system for Sphingomonads. *Appl. Environ. Microbiol.* **78**, 3774–3777. <https://doi.org/10.1128/AEM.07347-11> (2012).
40. Johnson, M. *et al.* NCBI BLAST: A better web interface. *Nucleic Acids Res.* **36**, W5–9. <https://doi.org/10.1093/nar/gkn201> (2008).
41. Sievers, F. *et al.* Fast, scalable generation of high-quality protein multiple sequence alignments using Clustal Omega. *Mol. Syst. Biol.* **7**, 539. <https://doi.org/10.1038/msb.2011.75> (2011).
42. Li, W. *et al.* The EMBL-EBI bioinformatics web and programmatic tools framework. *Nucleic Acids Res.* **43**, W580–584. <https://doi.org/10.1093/nar/gkv279> (2015).

Acknowledgements

This work was supported by JSPS KAKENHI Grant Nos. 15H04473 (E.M.), 19H02867 (E.M.), 19J11312 (M.F.), and 21J00894 (M.F.). Part of this work resulted from using research equipment shared in MEXT Project for promoting public utilization of advanced research infrastructure (Program for the SHARE, GIGAKU-Innovation Equipment Sharing Network) at Nagaoka University of Technology, Grant No. [JPMXS0430300121].

Author contributions

E.M. supervised the project. M.F., N.K., and E.M. designed the study and wrote the manuscript. M.F. performed the experiments with the following exceptions. S.Y. and K.S. analyzed PR, DCA, and AV conversion by *tonB1* mutants and overexpression strains of the *tonB1* operon genes. M.K. and M.F. performed FE-SEM analysis. S.H. synthesized DCA, PR, and HMPPD. S.Y. performed a statistical analysis of the conversion of lignin-derived aromatic compounds by overexpression strains of the *tonB1* operon genes. S.Y. and K.S. helped to interpret the data and discussed the results. All authors read and approved the manuscript.

Competing interests

The authors declare no competing interests.

Additional information

Supplementary Information The online version contains supplementary material available at <https://doi.org/10.1038/s41598-021-01756-8>.

Correspondence and requests for materials should be addressed to E.M.

Reprints and permissions information is available at www.nature.com/reprints.

Publisher's note Springer Nature remains neutral with regard to jurisdictional claims in published maps and institutional affiliations.



Open Access This article is licensed under a Creative Commons Attribution 4.0 International License, which permits use, sharing, adaptation, distribution and reproduction in any medium or format, as long as you give appropriate credit to the original author(s) and the source, provide a link to the Creative Commons licence, and indicate if changes were made. The images or other third party material in this article are included in the article's Creative Commons licence, unless indicated otherwise in a credit line to the material. If material is not included in the article's Creative Commons licence and your intended use is not permitted by statutory regulation or exceeds the permitted use, you will need to obtain permission directly from the copyright holder. To view a copy of this licence, visit <http://creativecommons.org/licenses/by/4.0/>.

© The Author(s) 2021